

EXPLAINING THE ENERGETIC AGN OUTBURST OF MS0735+7421 WITH MASSIVE SLOW JETS

Assaf Sternberg¹, Noam Soker¹

ABSTRACT

By conducting axisymmetrical hydrodynamical numerical simulations (2.5 dimensional code) we show that slow, massive, wide jets can reproduce the morphology of the huge X-ray deficient bubble pair in the cluster of galaxies MS0735+7421. The total energy of the jets, composed of the energy in the bubble pair and in the shock wave, is constraint by observations conducted by McNamara et al. (2009) to be $\sim 10^{62}$ erg. We show that two opposite jets that are active for ~ 100 Myr, each with a launching half opening angle of $\alpha \simeq 70^\circ$, an initial velocity of $v_j \sim 0.1c$, and a total mass loss rate of the two jets of $\dot{M}_{2j} \sim 100M_\odot \text{ yr}^{-1}$, can account for the observed morphology. Rapidly precessing narrow jets can be used instead of wide jets. In our model the cluster suffered from a cooling catastrophe ~ 100 Myr ago. Most of the mass that cooled, $\sim 10^{10}M_\odot$, was expelled back to the intracluster medium (ICM) by the AGN activity and is inside the bubbles now, $\sim 10\%$ formed stars, and $\sim 10\%$ of the cold gas was accreted by the central black hole and was the source of the outburst energy. This type of activity is similar to that expected to occur in galaxy formation.

Subject headings: galaxy clusters: cooling flows –Active Galactic Nuclei: individual (MS0735.6+7421).

1. INTRODUCTION

Many clusters of galaxies harbor bubbles (cavities) devoid of X-ray emission, e.g., Hydra A (McNamara et al. 2000), A 2597 (McNamara et al. 2001), RBS797 (Schindler et al. 2001), Abell 496 (Dupke & White 2001), Abell 4059 (Heinz et al. 2002), Perseus (Fabian et al. 2000) and Abell 2052 (Blanton et al. 2001, 2009). These low density bubbles are inflated by jets launched by the active galactic nuclei (AGN) sitting at the centers of these clusters. The

¹Department of Physics, Technion–Israel Institute of Technology, Haifa 32000, Israel; phassaf@techunix.technion.ac.il; soker@physics.technion.ac.il

properties of these jets are poorly understood. Although in most cases radio jets are observed to be associated with X-ray deficient bubbles, there is no general one-to-one correspondence between the radio jets and bubbles. In Abell 2626 (Rizza et al. 2000; Wong et al. 2008) and in Hercules A (Nulsen et al. 2005; Gizani & Leahy 2003), for example, no X-ray deficient bubbles are observed at the locations of strong radio emission.

The bubbles we are aiming to understand have their width not much smaller, and even larger, than their length; we term them ‘fat bubbles’. In previous papers (Sternberg et al. 2007; Sternberg & Soker 2008a,b) it has been shown that large bubbles can be inflated by slow-massive-wide (SMW) jets. Typical values are $v_j \sim 10^4 \text{ km s}^{-1} \sim 0.02 - 0.1c$, for the initial jet speed, $\dot{M}_{2j} \sim 1 - 50 M_\odot \text{ yr}^{-1}$ for the mass loss rate into the two jets, and a half opening angle of $\alpha \gtrsim 30^\circ$. Precessing narrow jets have the same effect as wide jets (Sternberg & Soker 2008a). In contrast to these simulated wide jets, synchrotron emission, mainly in radio and in synchrotron self-Compton X-ray and optical emission (e.g., Cygnus A, Wilson et al. 2000), show relativistic jets to be narrow. For that, it was argued, e.g., Binney (2004), that in many cases the relativistic jets carry a small fraction of the mass and energy in the outflow.

In this paper we continue with the view held in our previous papers, that radio jets do not necessarily trace the main energy and mass carried by the outflow from the AGN vicinity, neither in the period of activity nor in the outflow geometry. We apply this conjecture to the energetic outburst of the cluster MS0735.6+7421 (hereafter MS0735), where the bright radio jets reside inside the bubbles, but do not follow their exact geometry (McNamara et al. 2005). The very large bubbles in this cluster demand that the jets which inflated them were extremely energetic (Gitti et al. 2007). The lack of strong AGN emission and a low upper limit on present star formation rate, motivated McNamara et al. (2009) to propose that the jets were powered by the rotational energy (spin) of the central black hole (BH). They cite the model of Meier (1999, 2001), in which the dominant energy source of the jets is claimed to be the spinning BH. However, it is questionable whether the energy supplied by the spinning BH can exceed by much (or at all) the energy supplied by the accretion process (Livio et al. 1999; Li 2000)

We use only wide (or precessing jets) because narrow jets expand to large distances before they inflate large bubbles. This is clearly seen in figure 1 of Sternberg et al. (2007), where a jet with a half opening angle of 20° inflates a long narrow bubble rather than a more spherical bubble. Analytical arguments for wide jets are given in Soker (2004). In figure 2 of Sternberg & Soker (2008a) it can be seen that when a narrow jet precesses too close to the symmetry axis (15° in that case), it inflates a long bubble, rather than a large one as desired here.

In this paper we propose that the bubbles in MS0735 were inflated by SMW, or precessing, jets in an outburst that has ceased t_Q years ago, where t_Q is of the order of a few 10^7 yr. The energy came from the accretion process and not from the spinning BH. The present radio activity is a weak leftover from that eruption. The proposed scenario is outlined in §2, and implication for feedback in galaxy formation is discussed. The numerical method and initial conditions are described in §3, and the results of the numerical simulations are presented in §4. Our discussion and summary are in §5.

2. THE ENERGETIC OUTBURST OF MS0735

The bubble pair in MS0735 that we try to model is presented in Figure 1 (taken from McNamara et al. 2009, with some scaling added).

McNamara et al. (2009) estimated the total energy of the outburst in MS0735, i.e., both in the bubbles and the shocks, to be $E_{2j} = 1.2 \times 10^{62}$ erg, about half of it in the bubble and the rest in the outer shock wave. This estimate is based on the jet material being relativistic, i.e., $\gamma = 4/3$. For jets of non-relativistic material, i.e., $\gamma = 5/3$, the energy in the bubble is $\sim 4 \times 10^{61}$ erg, and the total energy estimate is $E_{2j} \simeq 10 \times 10^{61}$ erg. We will run jets with a total energy of $E_{2j} = 7.2 \times 10^{61}$ erg. For an efficiency of $\epsilon = 0.1$ of converting accretion energy to jets' power, the total accreted mass required to inflate the bubbles is $M_{\text{acc}} \simeq 4 \times 10^8 M_\odot$. This amount of accreted mass holds even if the jets are relativistic, as long as one does not make use of the energy stored in the spin of the BH. To account for this energy and accreted mass, we propose that the high activity (energetic) phase lasted for a time period of $\Delta t_H \sim 10^8$ yr that has ended t_Q (a few 10^7) years ago. During the time period t_Q the AGN activity has continued, but with a much lower power, about equal to the present power of the radio jets, and no star formation took place. In our model the jets that inflated the bubbles—the inflating jets—were slow, i.e., highly non-relativistic with $v_j \simeq 0.1c$, and massive, i.e., the mass outflow rate was much higher than the mass accretion rate. Feedback heating of cooling flow clusters with massive slow jets was studied before (Pizzolato & Soker 2005a; Soker & Pizzolato 2005; Sternberg et al. 2007). The total mass carried by the two jets is derived from the assumption that the kinetic energy of the jets is converted to the total energy in the bubbles and shocks, and it gives

$$M_{2j} = 8.4 \times 10^9 \left(\frac{E_{2j}}{7.5 \times 10^{61} \text{ erg}} \right) \left(\frac{v_j}{0.1c} \right)^{-2} M_\odot. \quad (1)$$

We emphasize that in *mass loss rate in the jets* or *total mass carried by the jets* we mean both the jet material and the material advected onto it. Basically, the BH itself ejected relativistic jets. However, within a short distance from the center, $r < 1$ kpc, they interacted with the

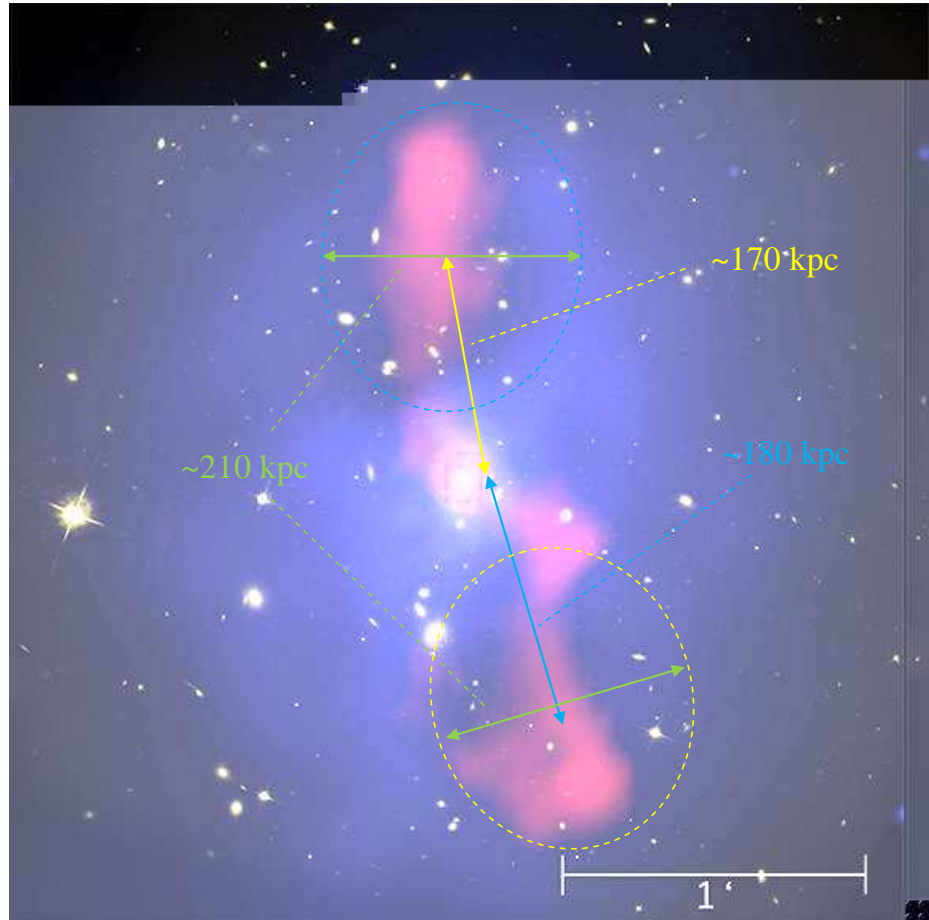


Fig. 1.— X-ray image of the bubble-pair in MS0735.6+7421 cluster (from McNamara et al. 2009). Image of the inner 200 arcsec (700 kpc) combining the X-ray (blue), I-band (white), and radio wavelengths (red). The two-sided arrow lines with different lengths and the dashed ellipses are added to allow comparison with the numerical results.

dense cooling gas, and formed SMW jets (Soker 2008).

Based on a UV power of $1.82 \pm 0.14 \times 10^{42}$ erg s $^{-1}$ in the 1800 – 2600Å band, McNamara et al. (2009) deduced a present day star formation rate of $\dot{M}_{\text{present}} = 0.25 M_{\odot}$ yr $^{-1}$. To estimate the mass that was converted to stars $\Delta t_H + t_Q \simeq 10^8$ yr ago we use figure 1 from Fioc & Rocca-Volmerange (1997). In that figure Fioc & Rocca-Volmerange (1997) give the spectral evolution after an instantaneous burst of star formation. The 1800 – 2600Å specific flux at 10^8 yr after a star formation burst can be fitted with $F_{\lambda} = 7 \times 10^{30} (\lambda/2000\text{\AA})^{-3/2}$ erg s $^{-1}$ Å $^{-1} M_{\odot}^{-1}$. Integrating in the 1800 – 2600Å band, we find that a flux of $1.82 \pm 0.14 \times 10^{42}$ erg s $^{-1}$ implies a total star formation mass of $3.7 \times 10^8 M_{\odot}$ (assuming a negligible present star formation rate) 10^8 yr ago. As the star formation rate was continuous and ended $\sim 10^8$ yr ago, we can take the average star formation time to be $\gtrsim 1.5 \times 10^8$ yr ago, and the total stellar mass that formed in the outburst to be larger $M_{\text{stars}} \sim 10^9 M_{\odot}$.

We use the above values to propose the following scenario for the inflation of the bubbles in MS0735. For a time period of $\sim 10^8$ yr, a cooling rate of $\sim 100 M_{\odot}$ yr $^{-1}$ result in a mass of $\sim 10^{10} M_{\odot}$ flowing toward the center of MS0735. Some of the cool mass might have come from a merger event. However, we basically propose that MS0735 went through a phase that might be termed a cooling catastrophe. The strong AGN activity ejected most of the cooling mass before much star formation occurred. A vigorous termination of star formation is needed in galaxy formation as well, where the expelled mass can be ~ 10 times the mass that converted to stars (e.g., Bower et al. 2008). The process we propose here might resemble the process that terminated star formation after the main phase of galaxies assembly.

There are three possible reasons that make the accretion and jet ejection that took place during the outburst of M0735 different than those during the main assembly phase of galaxies and their central BH. First, in MS0735 the central BH is an ultra-massive one (McNamara et al. 2009). This might lead to a high accretion rate that results in very strong jets, that ejected a large fraction of the cooling gas back to large radii. Second, the cooling catastrophe occurred after a hot dense ICM was built up in the cluster, such that large quantities of gas could cool, disturb the relativistic jets, and form slower, denser, and wider jets (Soker 2008). Third, most likely there is a massive BH companion to the central BH of MS0735 (Pizzolato & Soker 2005b). The evidence for precession is the point symmetric structure of the lobes. Pizzolato & Soker (2005b) considered a case of a BH companion of a mass $\sim 10\%$ the mass of the central BH, and at a distance of a few pc.

A small fraction, $\sim 5\%$, of the cooling mass was accreted by the BH, summing to a total of $M_{\text{acc}} \simeq 4 \times 10^8 (\epsilon/0.1)^{-1} M_{\odot}$, and a similar mass, $M_{\text{stars}} \sim 10^9 M_{\odot}$, was converted to stars. However, the huge amount of cool material near the center disturbed the relativistic jets blown by the BH within a short distance from the center, < 1 kpc. The mass that

disrupted the propagation of the jet was $\gtrsim 100$ times larger than the mass in the primary relativistic jets. This condition leads to an efficient transfer of energy from the relativistic jets to the disrupting gas, and the formation of slow massive wide (SMW) jets (Soker 2008). The material in the massive jets resides now inside the two bubbles, after it was heated when it was shocked. Both mass and energy are ingredients in the feedback heating of this cluster, as was suggested in the moderate cooling flow model (Pizzolato & Soker 2005a; Soker & Pizzolato 2005; Soker 2006).

The parameters of the proposed model are summarized in Table 1. Some of these parameters are used explicitly in the numerical simulations to be described in the next section (they are marked by an asterisk). With several numerical trials not presented here, we found that an active phase duration of $\sim 10^8$ yr can reproduce the observations. We took a round number of 10^8 yr. Much longer active phase will result in bubbles that have time to buoy to too large distances, and a too short active phase requires very high mass outflow rate, that pushes its way too fast along the symmetry axis. We then continue the bubble evolution for a time t_Q until it matches observations. As there are uncertainties in the velocity (hence mass loss rate) of the wide jets to be used in our model, we simulated three different cases, named Model I, II, and III.

Table 1: Model Parameters

	Symbol	Model I	Model II	Model III
Jet's half opening angle*	α	70°	70°	70°
Mass loss rate in both jets* (M_\odot yr $^{-1}$)	\dot{M}_{2j}	242.4	60.6	26.9
Jet's velocity*	v_j	$0.0576c$	$0.1152c$	$0.1727c$
Power of both jets* (10^{46} erg s $^{-1}$)	\dot{E}_{2j}	2.28	2.28	2.28
Duration of active phase*	Δt_H	10^8 yr	10^8 yr	10^8 yr
Time since end of active phase*	t_Q	2.5×10^7 yr	1.5×10^7 yr	1.5×10^7 yr
Total injected energy (10^{61} erg)	E_{2j}	7.2	7.2	7.2
Total injected mass ($10^9 M_\odot$)	M_{2j}	24	6.1	2.7
Total accreted mass by the BH ($10^9 M_\odot$)	M_{acc}	$0.4(\epsilon/0.1)^{-1}$	$0.4(\epsilon/0.1)^{-1}$	$0.4(\epsilon/0.1)^{-1}$
Total stellar mass formed ($10^9 M_\odot$)	M_{stars}	~ 1	~ 1	~ 1

Parameters that are marked by * are those used explicitly in the the numerical simulations. ϵ is the energy production efficiency of the accreting central BH.

Few words are appropriate here about the high mass loss rate we use in the simulations. In our previous papers we gave the supporting arguments for using such a high mass loss rate. What we like to emphasize here is that we use wide (or precessing; Sternberg & Soker 2008a) jets with high mass loss rates based on physical considerations (Soker 2004; Sternberg et al. 2007; Sternberg & Soker 2008a), and not from numerical limitations. In recent years

several papers have used jets with very high mass loss rates (e.g., Simionescu et al., 2009). Such high mass outflow rates must come with an appropriate physical discussion.

The total BH accreted mass of $\sim 4 \times 10^8 M_\odot$ is not a concern, as the BH in MS0735 is super massive, $M_{\text{BH}} \simeq 5 \times 10^9 M_\odot$, and possibly even $M_{\text{BH}} \gtrsim 10^{10} M_\odot$ (McNamara et al. 2009).

3. NUMERICAL METHODS AND INITIAL CONDITIONS

The simulations were performed using the *Virginia Hydrodynamics-I* code (VH-1; Blondin et al. 1990; Stevens et al. 1992), as described in Sternberg & Soker (2008b). In this paper we mention only the important features of the code.

Gravity was included in the form of a constant gravitational potential of a dark matter halo using the NFW profile (Navarro et al. 1996),

$$\Phi_{\text{NFW}}(r) = 4\pi r_s^2 \delta_c \rho_{\text{crit}} G \left[1 - \frac{\ln(r/r_s + 1)}{r/r_s} \right], \quad (2)$$

where $r_s = \frac{r_v}{c}$ is a scale radius, $r_v = 1700$ kpc is the virial radius, $c = 3.45$ is the concentration factor, $\delta_c = \frac{200}{3} \frac{c^3}{\ln(1+c) - \frac{c}{1+c}}$, and $\rho_{\text{crit}} = \frac{3H^2}{8\pi G}$ is the critical density of the Universe at $z = 0$. The ICM gas was set in hydrostatic equilibrium,

$$\rho_{\text{gas}}(r) = \rho_{\text{gas},0} e^{-b} \left(\frac{r}{r_s} + 1 \right)^{\frac{b}{r/r_s}}, \quad (3)$$

with $b \equiv 4\pi r_s^2 \delta_c \rho_{\text{crit}} \mu m_p G / k_B T_v$, M_v is the virial mass, and $T_v = \frac{\gamma G \mu m_p M_v}{3k_B r_v} = 5.7 \times 10^7$ K is the virial temperature, which is the average temperature given by Gitti et al. (2007) for the relevant area simulated in our simulations. The central density was set to $\rho_{\text{gas},0} = 1.9 \times 10^{-26}$ g cm⁻³. Radiative cooling was not included.

We study a three-dimensional axisymmetric flow with a 2D grid (referred to as 2.5D). Our computational domain was $r \in [1, 400]$ kpc and $\theta \in [0, \pi/2]$. Hence, we simulate a quarter of the meridional plane using the two-dimensional version of the code in spherical coordinates. The symmetry axis of all plots shown in this paper is along the x (horizontal) axis. The y axis is the equatorial plane. Reflective boundary conditions were implemented at the symmetry axis, i.e., $\theta = 0$, and at the equatorial plane, i.e., $\theta = \pi/2$. At the inner and outer radii an inflow/outflow boundary condition was implemented, i.e., matter was free to flow in/out of the computational grid.

The point-symmetric morphology of the bubbles in MS0735 suggest that the inflating jets precessed. However, our 2.5D numerical code can only simulate precessing jets with a

very short rotation period around the symmetry axis. In our previous papers we have shown that the behavior of these jets is very similar to the behavior of wide jets. Therefore, we use wide jets in our simulations, with the understanding that rapidly precessing jets give similar results.

The jets were injected at a radius of 1 kpc, with a constant power of $\dot{E}_j = 1.14 \times 10^{46}$ erg s⁻¹ per one jet, and a constant radial velocity v_j , hence with a constant mass flux of $2\dot{E}_j/v_j^2$ per one jet, within a half opening angle of α . See Table 1 for the properties of the different jets we used.

4. NUMERICAL RESULTS

Figure 2 shows density maps (density given in log scale of g cm⁻³) of the evolution of the model I jet (see Table 1 for the jet’s parameters). The jet was turned off at $t = 100$ Myr, at which time a low density cavity with a radius of ~ 100 kpc has been inflated. For clarity, we note that by *the bubble* we mean the shocked jet material, i.e., the bubble does not include the jet material before the reverse shock situated at ~ 40 kpc. The bubble continues to rise and buoy outward from the cluster center.

At $t = 125$ Myr the bubble’s center resides at a distance of ~ 170 kpc from the cluster center. At this time the bubble is a bit elongated with a major axis of ~ 220 kpc and a minor axis of ~ 180 kpc. The ratio between the density of the matter inside the bubble, ρ_{bub} , and the density of the surrounding ICM, ρ_{ICM} , is $\rho_{\text{bub}}/\rho_{\text{ICM}} \sim 0.1 - 0.01$. The forward shock is elliptical and located at ~ 330 kpc near the symmetry axis and at ~ 240 kpc near the equatorial plane. The shock eventually decays into a sound wave. However, at the end of our calculation it is still a shock wave.

The arrows given in the bottom panel of Fig. 2 represent the velocities. The arrows represent four velocity bins: (i) $0.1c_s \leq v_j \leq c_s$ (shortest arrows); (ii) $c_s \leq v_j \leq 7.5c_s$; (iii) $7.5c_s \leq v_j \leq 15c_s$; (iv) $15c_s \leq v_j \leq 30c_s$ (longest arrows), where $c_s = 1152$ km s⁻¹ is the unperturbed ICM speed of sound. Figure 3 shows the temperature map of this bubble at the same times. The matter inside the bubble has a temperature of about an order of magnitude higher than that of the surrounding ICM. The temperature map taken at $t = 100$ Myr clearly shows the distinction between the pre-shocked jet material and the shocked jet material, i.e., the bubble.

Figures 4 and 5 show density and temperature maps, respectively (log scales) of the evolution of both a model II jet (left panels) and a model III (right panels) jet. The model III jet has a higher velocity and lower mass loss rate compared to model II, but the same

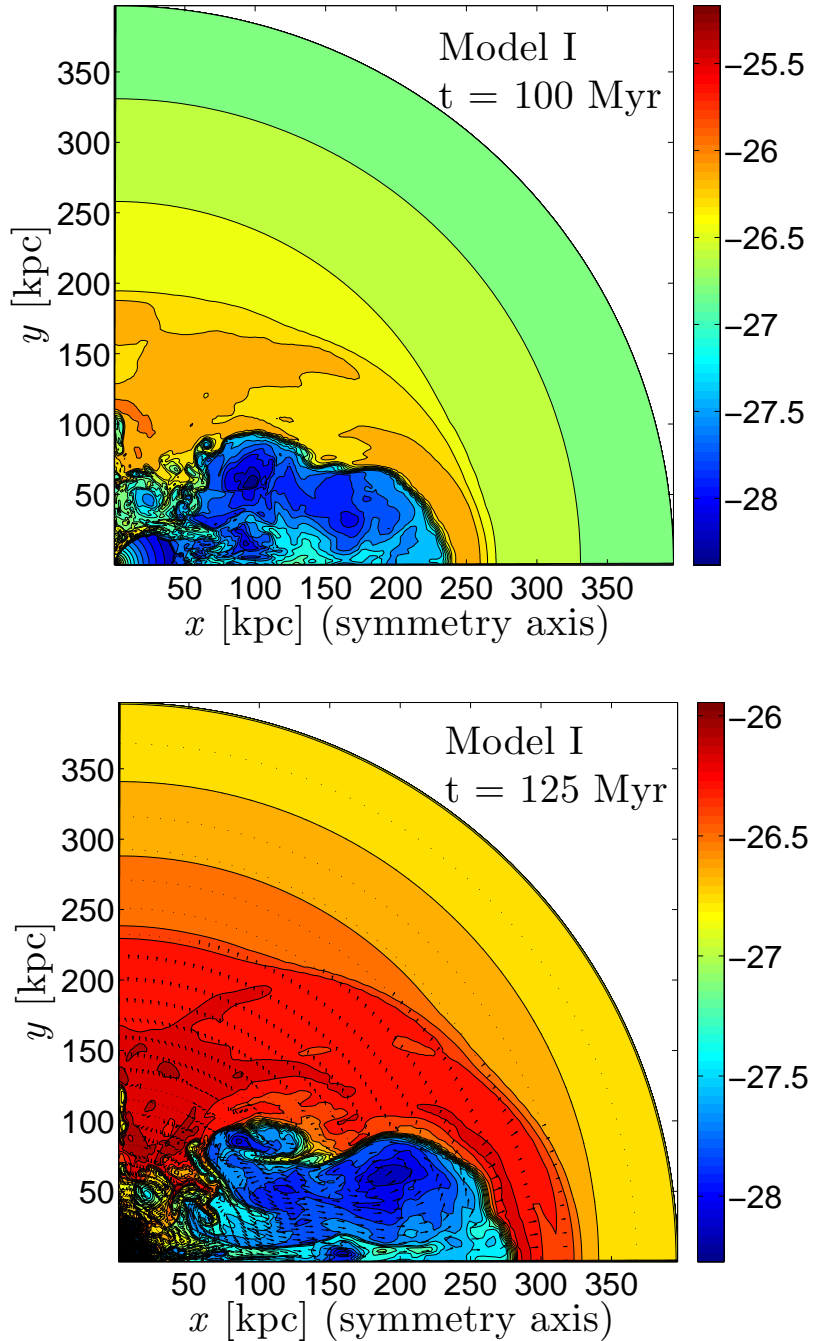


Fig. 2.— Log-density maps of the evolution of the model I jet at $t = 100$ Myr and at $t = 125$ Myr, as indicated in the figures. The jet was active for 100 Myr and was turned off at $t = 100$ Myr. The density is given in $\log(\text{g cm}^{-3})$. The arrows drawn in the bottom panel represent the flow velocity, and are grouped into four velocity bins: (i) $0.1c_s \leq v_j \leq c_s$ (shortest arrows); (ii) $c_s \leq v_j \leq 7.5c_s$; (iii) $7.5c_s \leq v_j \leq 15c_s$; (iv) $15c_s \leq v_j \leq 30c_s$ (longest arrows), where $c_s = 1152 \text{ km s}^{-1}$ is the unperturbed ICM speed of sound.

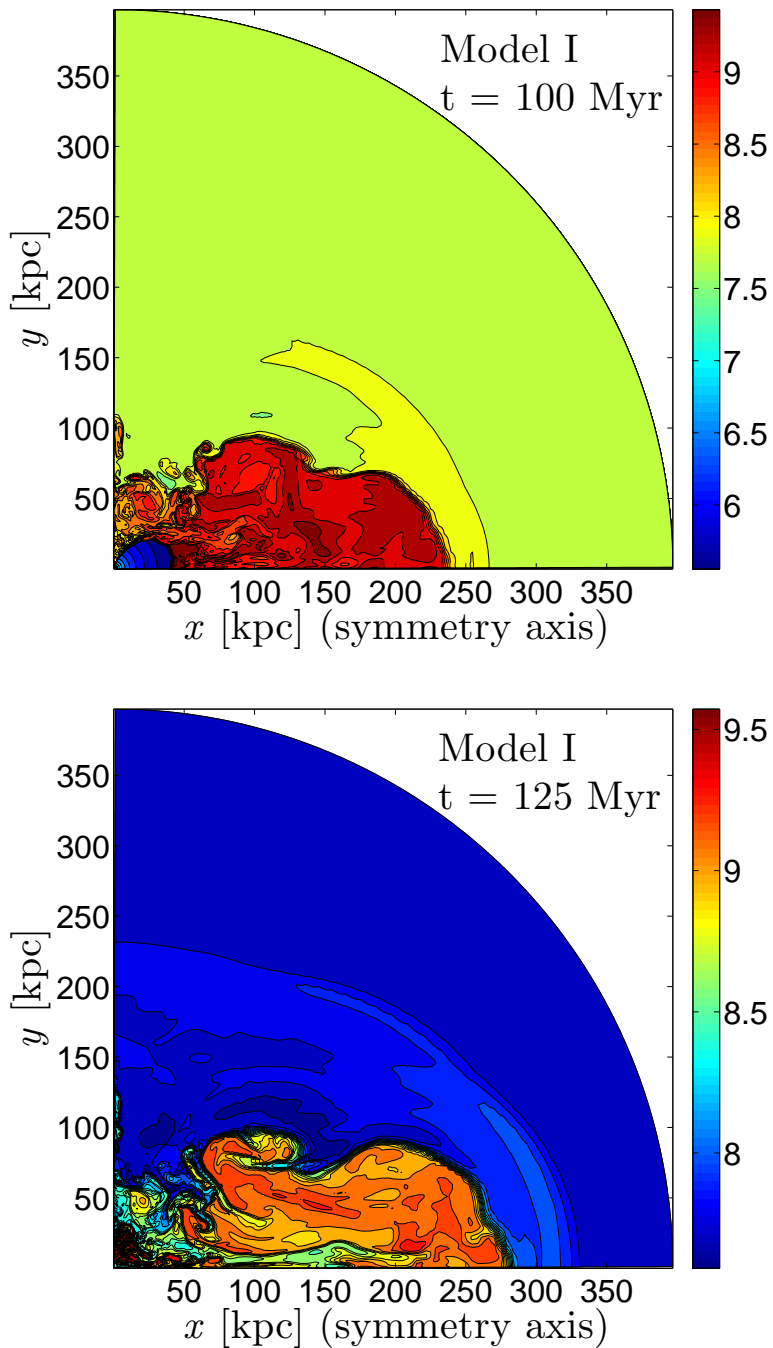


Fig. 3.— Log-temperature map of the bubble inflated by the model I jet at $t = 100$ Myr and $t = 125$ Myr. The temperature is given $\log(K)$.

power and the same initial opening angle (see Table 1 for properties of both jets). As in model I, in each case the jet was active for $t = 100$ Myr. In both models II and III the jets have inflated low density bubbles attached to the center. These bubbles are comparable to the one inflated by the model I jet, though, they are more elongated and the back flow of low density matter toward the equatorial plane is more pronounced. The evolution of the bubbles were followed for another 15 Myr.

At $t = 115$ Myr, as seen in the bottom left panel of Fig. 4, the model II bubble’s center is at a distance of ~ 175 kpc from the center. The bubble is elongated with a major axis of ~ 250 kpc and a minor axis of ~ 170 kpc. The shock front is elliptical and is located at ~ 330 kpc near the symmetry axis and at ~ 220 kpc near the equatorial plane.

At $t = 115$ Myr, as seen in the bottom right panel of Fig. 4, the model III bubble’s center is at a distance of ~ 180 kpc from the cluster center. It is more elongated than the bubbles inflated in the models I and II. It’s major axis is ~ 240 kpc and it’s minor axis is ~ 150 kpc. There is a non-negligible amount of low density matter near the equatorial plane. The front shock is elliptical, as it is in the other models, and it is located at $r = 320$ kpc along the symmetry axis, and $r = 220$ kpc in the equatorial plane.

The bubbles entrain cold gas into them. Most notable is Model III at $t = 115$ Myr, where tongues of denser gas are seen to penetrate the bubble. It is most likely that small scale mixing and heat conduction will mix this gas with the hot bubble gas. Our numerical code cannot handle these small scale processes. The entrained gas will reduce somewhat the bubble average temperature, but not to a degree that can be explored with present observations. In any case, this process is desirable, as it is one of the channels by which the bubbles can heat the ICM.

5. DISCUSSION AND SUMMARY

The center of the north and south bubbles in MS0735 reside at distances of ~ 170 kpc and ~ 180 kpc from the cluster center, respectively, and have a radius of ~ 105 kpc (Gitti et al. 2007; see Fig. 1 here). The actual numbers may vary due to projection effects. The model I jet inflates a bubble, that if left to rise buoyantly for 25 Myr, has both size and location that is in good agreement with the bubbles of MS0735. This is clearly seen in Figure 2. None the less, there are discrepancies between our results and the observations. A minor discrepancy is in the location of the shock front. Observations show the shock front to be elliptical with a semimajor axis of ~ 360 kpc and a semiminor axis of ~ 240 kpc (Gitti et al. 2007). While our model I does indeed have an elliptical shock front with a semiminor axis

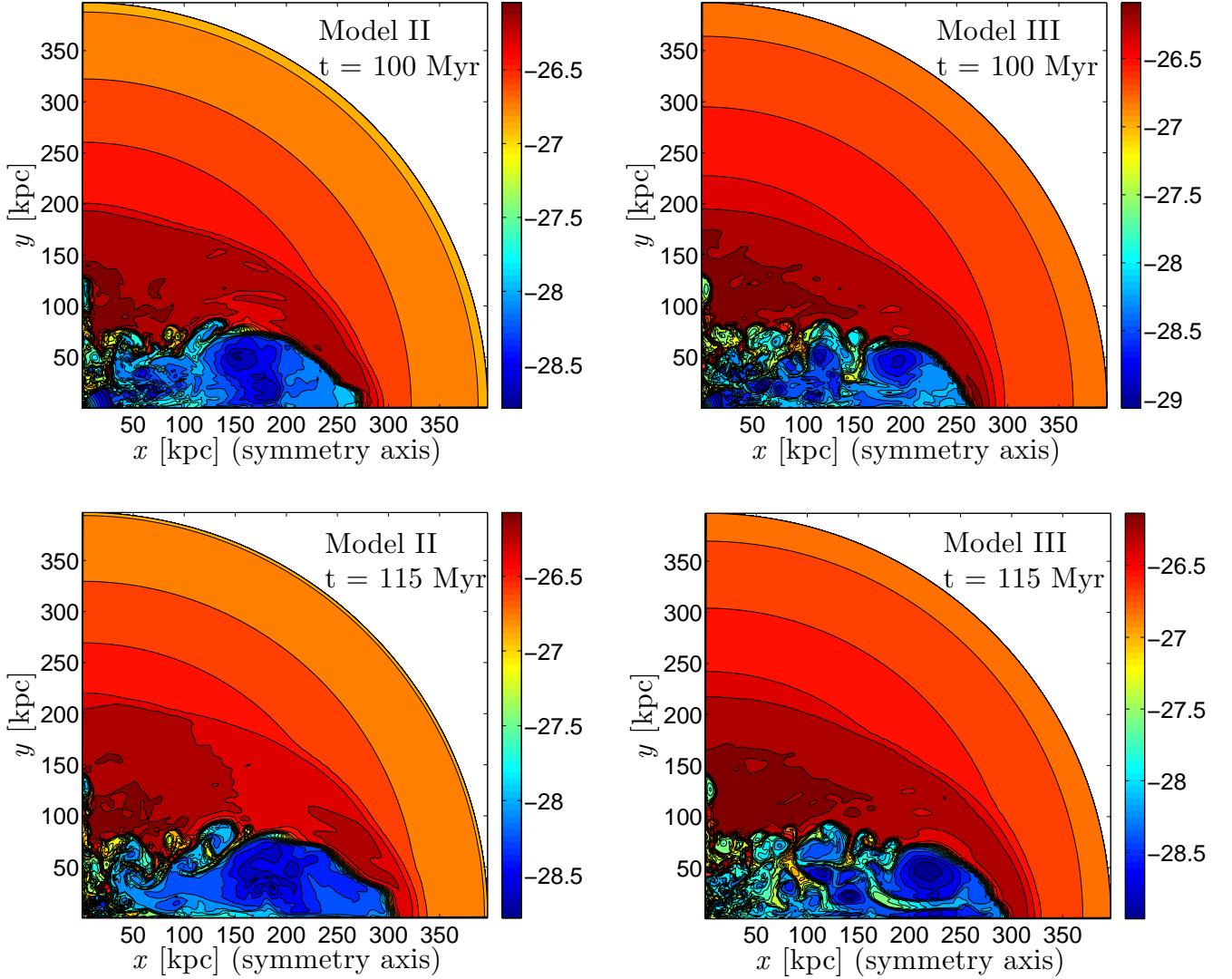


Fig. 4.— Log-density maps of the evolution of a model II jet (left panels) and a model III jet (right panels) shown at two different times (as indicated in the figures). In both cases the jet was turned off at $t = 100$ Myr. Note the mixing of dense material into the bubble. The density is given in $\log(g\text{ cm}^{-3})$.

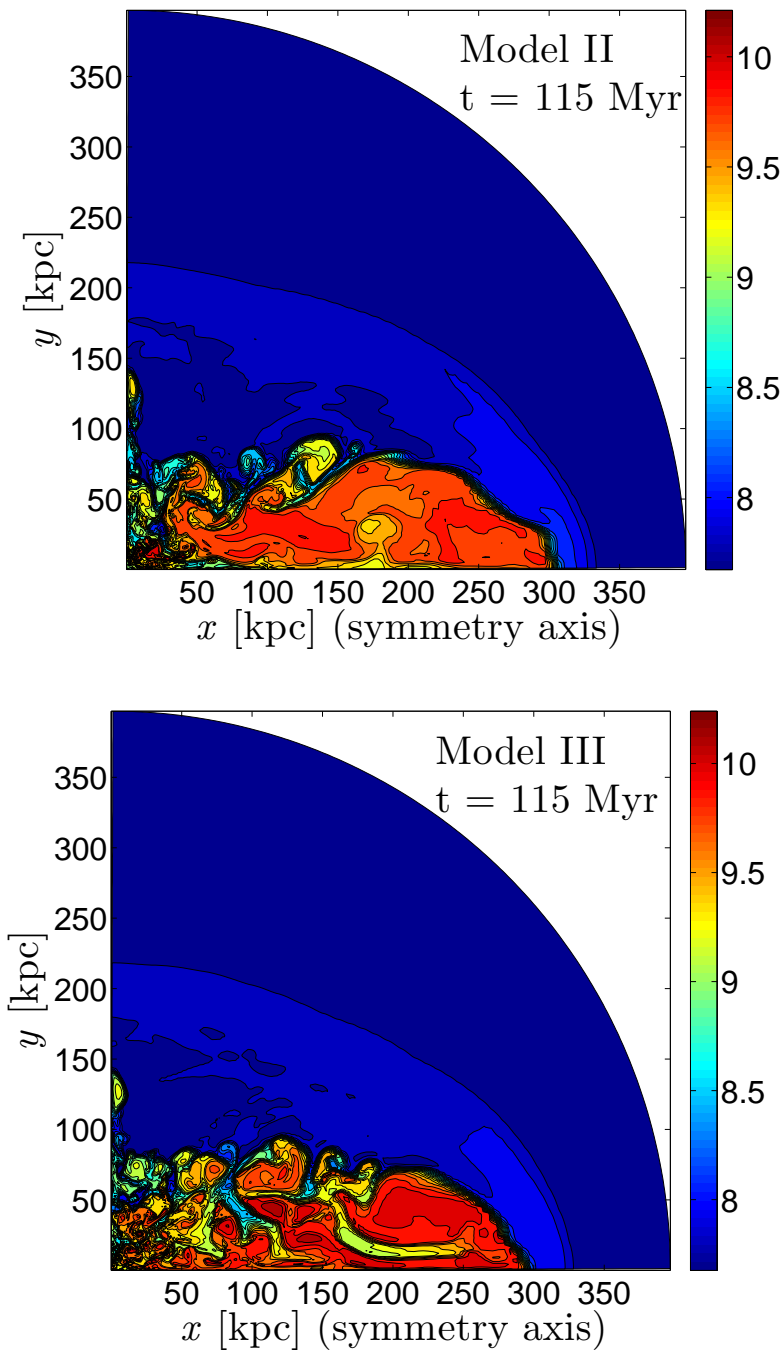


Fig. 5.— Log-temperature map of the bubbles inflated by the model II jet and a model III jet at $t = 115$ Myr. Note the mixing of cold and hot material inside the bubble. The temperature is given $\log(K)$.

of ~ 240 kpc it's semimajor axis is ~ 330 kpc. This discrepancy can be attributed to our cluster density profile that is not exactly as the real cluster density profile or to projection effects (e.g., jet axis not exactly in the plane of the sky).

A more serious discrepancy is in the non-negligible low density matter flow toward the equatorial plane that is present in our simulations but is not seen in the observations. Three effects that are not included in our simulations might reduce the presence of the low density gas near the equatorial plane. (*i*) Including radiative cooling might bring more cooler gas to fall near the equator replacing some of the hot gas. (*ii*) The turbulent flow near the equator close to the center will stretch magnetic field lines. In response, the magnetic tension might limit the back flow. It has been shown in numerical simulations that magnetic fields can prevent small scale mixing and instabilities, which can prevent some of the backflow. (e.g., Brüggen & Kaiser 2001; Jones & De Young 2005; Ruszkowski et al. 2007; Robinson et al. 2004). We note that magnetic fields are not required to stabilize the bubble against perturbations on large scales (Sternberg & Soker 2008b); magnetic fields might help in stabilizing against short wavelength perturbations by supplying tension. (*iii*) Accurate treatment of turbulence and mixing, such as in the subgrid model of Scannapieco & Brüggen (2008; also Brüggen et al. 2009), might prevent some of the back flow. These effects will have to be studied in future simulations.

The results of model II and III are less compatible with the observations. If some of the effects mentioned above are included, it is possible that model II with a total outflow rate of $\dot{M}_{2j} \simeq 50M_{\odot} \text{ yr}^{-1}$ can match observations. Precessing jets can also allow somewhat faster jets (but still highly subrelativistic). The bubbles inflated using the models with the faster jets are rather elongated and the amount of low density matter flowing to the equatorial plane is more substantial. This supports our preference for rather slow, yet still highly supersonic, massive jets over the faster and less massive ones, as was also shown in Sternberg et al. (2007). None the less, the bubbles of MS0735 might not lie exactly perpendicular to our line of sight. If this is so, then the bubbles might be more elongated, making the results of models II and III more agreeable with the observations. It is also plausible that the bubbles of MS0735 were inflated by precessing jets and not by wide fixed jets. In that case, a narrow jet would rapidly precesses at different angle around the symmetry axis. The angle of the jet's axis relative to the symmetry axis of the bubbles would change from zero to $\sim 70^\circ$. As was shown in Sternberg & Soker (2008a), rapidly precessing slow and massive jets inflate bubbles similar to those inflated by SMW jets. Therefore, even if the jets are rapidly precessing, our model will still prefer slow and massive jets over faster and less massive ones.

We thank John Blondin for his immense help with the numerical code. We thank Craig Sarazin, Brian McNamara, Marcus Brüggen, Fabio Pizzolato, and an anonymous referee

for helpful comments. This research was supported by the Asher Fund for Space Research at the Technion, and the Israel Science Foundation.

REFERENCES

Binney, J. 2004, in The Riddle of Cooling Flows in Galaxies and Clusters of Galaxies, Eds. T. Reiprich, J. Kempner, and N. Soker, published electronically at <http://www.astro.virginia.edu/co> (astroph/0310222)

Blanton, E. L., Randall, S. W., Douglass, E. M., Sarazin, C. L., Clarke, T. E. & McNamara, B. R. 2009, *ApJ, Letters*, in press (arXiv:0904.1610)

Blanton, E. L., Sarazin, C. L., McNamara, B. R., & Wise M. W. 2001, *ApJ*, 558, L15

Blondin J.M., Kallman T.R., Fryxell B.A., Taam R.E. 1990, *ApJ*, 356, 591

Bower, R. G., McCarthy, I. G., & Benson, A. J. 2008, *MNRAS*, 390, 1399

Brüggen, M. & Kaiser, C. R., 2001, *MNRAS*, 325, 676

Brüggen, M., Scannapieco, E., & Heinz, S. 2009, *MNRAS* (arXiv:0902.4242)

Dupke, R., & White, R. E. III 2001, High Energy Universe at Sharp Focus: Chandra Science, ed. E. M. Schlegel & S. Vrtilek (San Francisco: ASP Conference Series), 51

Fabian, A. C., et al. 2000, *MNRAS*, 318, L65

Fioc, M., & Rocca-Volmerange, B. 1997, *A&A*, 326, 950

Gitti, M., McNamara, B. R., Nulsen, P. E. J., & Wise, M. W. 2007, *ApJ*, 660, 1118

Gizani, N. A. B., & Leahy, J. P. 2003, *MNRAS*, 342, 399

Heinz, S., Choi, Y.-Y., Reynolds, C. S., & Begelman, M. C. 2002, *ApJ*, 569, L79

Jones, T. W. & De Young, D. S. 2005, *ApJ* 624, 586

Li, L.-X. 2000, *PhRvD* 61, 4016

Livio, M., Ogilvie, G. I., & Pringle, J. E. 1999, *ApJ*, 512, 100

McNamara, B. R., Kazemzadeh, F., Rafferty, D. A., Birzan, L., Nulsen, P. E. J., Kirkpatrick, C. C., & Wise, M. W. 2009, *ApJ* (arXiv:0811.3020)

McNamara, B. R., Nulsen, P. E. J., Wise, M. W., Rafferty, D. A., Carilli, C., Sarazin, C. L., & Blanton, E. L. 2005, *Natur*, 433, 45

McNamara, B. R., Wise, M. W., Nulsen, P. E. J., et al. 2000, *ApJ*, 534, L135

McNamara, B. R., Wise, M. W., Nulsen, P. E. J., et al. 2001, *ApJ*, 562, L149

Meier, D. L. 1999, *ApJ*, 522, 753

Meier, D. L. 2001, *ApJ*, 548, L9

Navarro, J. F., Frenk, C. S., & White, S. D. M. 1996, *ApJ*, 462, 563

Nulsen, P. E. J., Hambrick, D. C., McNamara, B. R., Rafferty, D., Birzan, L., Wise, M. W., & David, L. P. 2005, *ApJ*, 625, L9

Pizzolato, F., & Soker, N. 2005a, *ApJ*, 632, 821

Pizzolato, F., & Soker, N. 2005b, *AdSpR*, 36, 762

Rizza, E., Loken, C., Bliton, M., Roettiger, K., Burns, J. O., & Owen, F. N. 2000, *AJ*, 119, 21

Robinson, K. et al. 2004, *ApJ*, 601, 621

Ruszkowski, M., Ensslin, T. A., Brüggen, M., Heinz, S., & Pfrommer, C. 2007, *MNRAS*, 378, 662

Scannapieco, E., & Brüggen, M. 2008, *ApJ*, 686, 927

Schindler, S., Castillo-Morales, A., De Filippis, E., Schwope, A., & Wambsganss, J. 2001, *A&A* 376, L27

Simionescu, A., Roediger, E., Nulsen, P.E. J., Brüggen, M., Forman, W. R., Böhringer, H., Werner, N., & Finoguenov, A. 2009 (arXiv:0810.0271)

Soker, N. 2004, *A&A*, 414, 943

Soker, N. 2006, *NewA*, 12, 38

Soker, N. 2008, *NewA*, 13, 296

Soker, N. & Pizzolato, F. 2005, *ApJ*, 622, 847

Sternberg, A., Pizzolato, F., & Soker, N. 2007, *ApJ*, 656, L5

Sternberg, A., & Soker, N. 2008a, *MNRAS*, 384, 1327 (2008a)

Sternberg, A., & Soker, N. 2008b, *MNRAS*, 389, L13 (2008b)

Stevens, I. R., Blondin, J. M., & Pollock, A. M. T. 1992, *ApJ*, 386, 265

Wilson, A. S., Young, A. J., & Shopbell, P. L. 2000, *ApJ*, 544, L27

Wong, K.-W. Sarazin, C. L., Blanton, E. L. & Reiprich, T. H. 2008, *ApJ*, 682, 155